Status of the CALET Ultra Heavy Cosmic Ray Analysis

Y. AKAIKE[1] AND B. F. RAUCH[2] FOR THE CALET COLLABORATION

1. University of Maryland Baltimore County and NASA Goddard Space Flight Center, Greenbelt, MD 20771, USA

2. Department of Physics and McDonnell Center for the Space Sciences, Washington University in St. Louis, St. Louis, MO 63130, USA

CALET supported by JAXA in Japan, ASI in Italy and in the USA by NASA grant #NNX11AE02G.

yosui.akaike@nasa.gov and *brauch@physics.wustl.edu*

Abstract

The CALorimetric Electron Telescope (CALET) was launched to the International Space Station (ISS) on August 19, 2015, and has been returning science data since October 13, 2015. Through the main calorimeter (CAL), CALET observes the fluxes of high-energy electrons, gamma rays and nuclei. CALET measures the energy spectra of the more abundant cosmic-ray nuclei through $_{26}$Fe passing within the full CAL geometry, and utilizing an ultra-heavy cosmic-ray (UHCR) trigger, measures the relative abundances of the rare UHCR nuclei through $_{40}$Zr with an expanded geometric acceptance. Preliminary analysis of the $_{26}$Fe statistics from the first ~ 13 months of CAL data passing the UHCR trigger have validated the preflight estimate that in a 5 year mission CALET will observe comparable UHCR statistics to those achieved in the first flight of the SuperTIGER balloon-borne UH experiment. The CALET UHCR measurements will complement those by SuperTIGER in a similar energy range without the need to correct for atmospheric interactions, as well as those at lower energy and with lower statistics by the space-based ACE-CRIS instrument. CALET is unique as an instrument sensitive to UHCR in having the dynamic range to measure from $_1$H to $_{40}$Zr. We present the status of the CALET UHCR analysis.

CALET Instrument and Main Objectives

The CALET instrument and its main scientific objectives are covered at this conference by Shoji Torii [1]. CALET consists of a Calorimeter (CAL) and a Gamma-ray Burst Monitor (CGBM) [2], which are shown on the left in Fig. 1. The side view of the CAL is shown on the right in Fig. 1, and consists of the following detectors:

- CHD: charge detection module composed of two crossed layers of 32 mm wide $\times$ 10 mm thick $\times$ 450 mm long EJ200 scintillator paddles.
- IMC: imaging calorimeter composed of eight x-y planes of 448 1 mm^2 scintillating fibers interleaved with 3 radiation lengths ($X_\circ$) of tungsten.
- TASC: total absorption calorimeter with twelve crossed layers of 16 PWO logs, each 19 mm wide $\times$ 20 mm tall $\times$ 326 mm long, for a total of 27 $X_\circ$ depth.

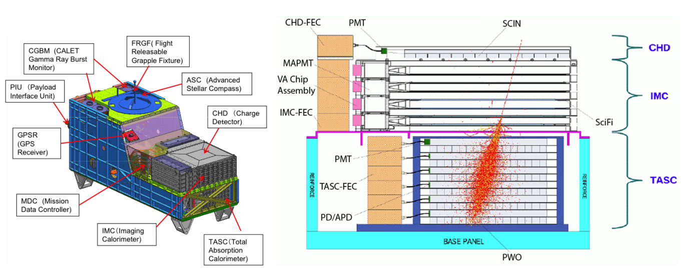

Figure 1: Left: CALET instrument package showing CAL and CGBM subsystems. Right: CAL side-view showing CHD, IMC, and TASC detectors with an example image of a simulated 1 TeV electron shower.

CALET measures:

- electrons with energies from 1 GeV to 20 TeV owing to the great depth of the CAL (30 $X_\circ$) [3, 4].
- gamma-rays energies between 10 GeV and 10 TeV [5, 6].
- nuclei $1 \le Z \le 40$ up to 1,000 TeV and energy spectra for $Z \le 28$ [7, 8].

Heavy and Ultra-Heavy Cosmic Rays

The left plot in Fig. 2 shows that UHCR yield important clues to the origins of cosmic rays [9, 10, 11] in:

- source composition including a contribution from material enhanced by massive star nucleosynthesis.
- acceleration mechanism with preferential acceleration of refractory elements.

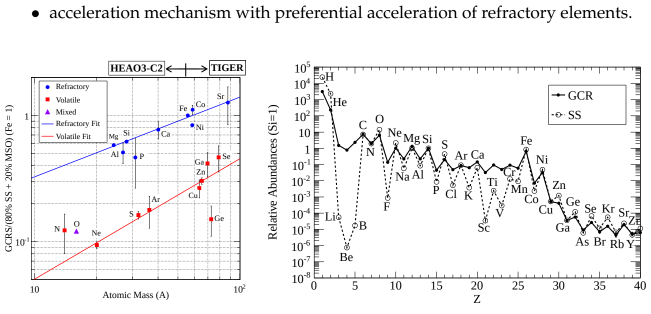

Figure 2: Left: Ratio of measured Galactic cosmic-ray source (GCRS) abundances ($Z \le 26$ from [12] and $26 \le Z$ from [9]) to mixture of 80% Solar System (SS) [13] and 20% massive star outflow (MSO) normalized to Fe=1 plotted against atomic mass. Right: SS [13] and GCR relative abundances at 2 GeV/nuc ($1 \le Z \le 2$ from [14], $Z = 3$ from [15], $4 \le Z \le 28$ from [12], $Z = 29$ from [9], and $28 \le Z \le 40$ from [10].) normalized to $_{14}$Si= 1.

The right plot in Fig. 2 compares Solar System (SS) and GCR relative abundances (Fe=1) at 2GeV/nuc, showing that UHCR ($Z \ge 30$) are very rare - putting a premium on collecting power.

UHCR Data Analysis

CALET data undergoes processing prior to distribution at the Waseda CALET Operations Center (WCOC) that prepares data for the international collaboration [16] and monitors CALET. Data preparation includes:

- correcting for variations in response over time and as a function of position within detector elements using minimum ionizing particles (MIPs) [17, 18].
- applying the energy scale calibration [19].
- determining event track reconstructions [20].

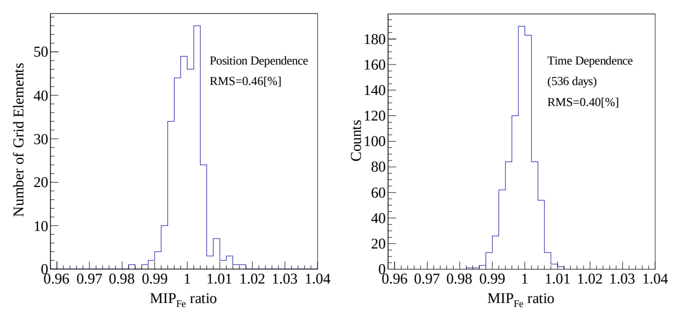

Figure 3: Left: Residual variation in $_{26}$Fe peak signal with position in the CHD in the preliminary UHCR analysis. Right: Residual variation in $_{26}$Fe peak signal with time in CHD in the preliminary UHCR analysis.

Additional steps for the CALET UHCR analysis include:

- selecting events passing UHCR trigger, requiring above threshold signals in the CHD and top 4 IMC layers.
- applying detector position dependent calibrations based on fits to the $_{26}$Fe peak, giving the residual variance shown on the left in Fig. 3.
- applying detector time dependent calibrations based on fits to the $_{26}$Fe peak, giving the residual variance shown on the right in Fig. 3.
- apply a CHDX and CHDY charge consistency cut to exclude events interacting in the CHD [8], shown on the left in Fig. 4.
- apply a charge assignment accounting for scintillator saturation following the method in [21], with the resulting preliminary UHCR charge histogram with the above corrections applied shown on the right in Fig.4.

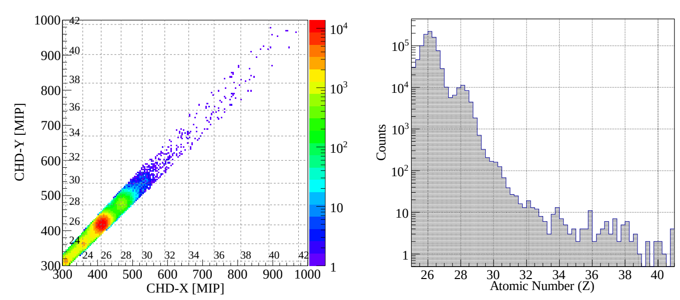

Figure 4: Left: CHDX and CHDY charge consistency cut [8]. Right: Preliminary CALET UHCR charge histogram with 4 bins/charge unit for UH trigger events within 60° of vertical and for a geomagnetic vertical cutoff rigidity > 4 GV.

Rigidity Cuts for ISS Orbit

Applying a geomagnetic rigidity based energy threshold cut can improve the CALET UHCR charge resolution by eliminating lower energy events where the scintillation signal varies most strongly with energy.

- Cutoff rigidity is the critical momentum, $p_{crit}(\gamma, \lambda)$ [22], divided by the atomic number $R_{cutoff} = p_{crit}(\gamma, \lambda)/Z$. Critical momentum as a function of geomagnetic latitude (λ) and East-West angle (γ) shown in Fig. 5 left:

$$p_{crit}(\gamma, \lambda) = 60Z \left[\frac{1 - \sqrt{1 - \cos(\gamma)\cos^3(\lambda)}}{\cos(\gamma)\cos(\lambda)} \right]^2.$$

- Geomagnetic latitude calculated from vertical cutoff rigidities ($R_{cut} = 15\cos^4(\lambda)$ GV [22]) at 450 km [23] in 1° longitude $\times$ 1° latitude bins shown in Fig. 5 right.
- Events above an energy threshold can be selected utilizing rigidity cut based on critical momentum with: $E_{crit} = \sqrt{p_{crit}^2/A^2 + m_{amu}^2} - m_{amu}$.
- Using an East-West angle based threshold cut will allow CALET to realize the potential of the larger UHCR trigger acceptance: geometry factor 0.44 m^{2}sr versus 0.07 m^{2}sr for events contained in the TASC.

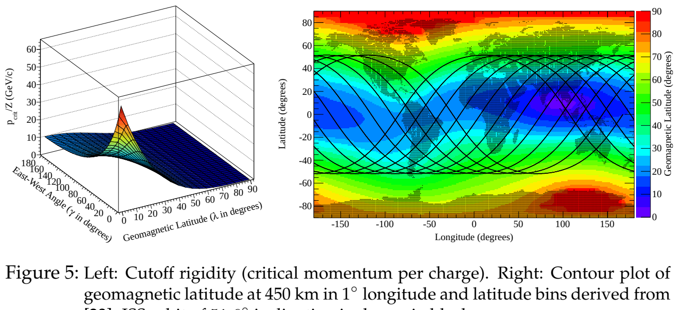

Figure 5: Left: Cutoff rigidity (critical momentum per charge). Right: Contour plot of geomagnetic latitude at 450 km in 1° longitude and latitude bins derived from [23]. ISS orbit of 51.6° inclination is shown in black curves.

Preliminary CALET UHCR Results

The preliminary analysis of the first 18 months of data shows that CALET can measure the UHCR.

- Fig. 6 left shows the charge histogram from Fig. 4 right with a multiple-Gaussian fit with fixed $\sigma = 0.35$ and integer means.
- The preliminary analysis has residual contamination from more-abundant lower-Z peaks that should be resolved with an improved angle-dependent geomagnetic energy threshold cut.

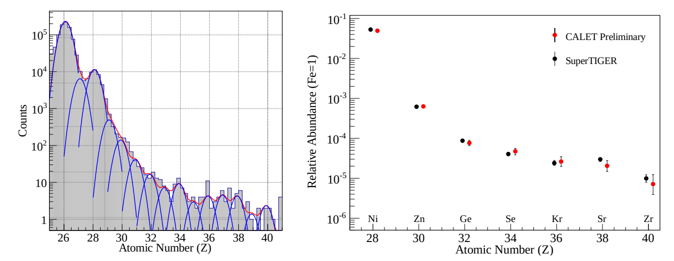

Figure 6: Left: Preliminary CALET UHCR charge histogram with 4 bins/charge unit for UH trigger events within 60° of vertical and for a geomagnetic vertical cutoff rigidity > 4 GV with multiple-Gaussian fit with fixed $\sigma = 0.35$ and integer means. Right: Even-Z relative abundances ($_{26}$Fe=1) for CALET (red points) with statistical errors only compared with SuperTIGER (black points) [10].

- Fig. 6 right shows the CALET UHCR even-Z relative abundances determined by summing events within ± 0.5 charge units (cu) of each element charge and deducting the background from Gaussian fits to the adjacent peaks compared with those from SuperTIGER [10].
- Preliminary CALET even-Z measurements agree to within the CALET statistical errors, but odd-Z abundances are still contaminated by spillover from more abundant adjacent elements.
- Predictions for CALET observing similar UHCR statistics to the first SuperTIGER flight in 5 years [24] validated by $_{26}$Fe statistics from preliminary analysis of the first ~ 13 months of CAL data passing the UHCR trigger agreeing with those predicted by the model to within 10%.

References

[1] S. Torii for the CALET Collaboration, in proceedings of *The 35th International Cosmic Ray Conference*, PoS (ICRC2017) (2017).

[2] K. Yamaoka for the CALET Collaboraiton, in proceedings of *The 35th International Cosmic Ray Conference*, PoS (ICRC2017) 614 (2017).

[3] Y. Asaoka for the CALET Collaboration, in proceedings of *The 35th International Cosmic Ray Conference*, PoS (ICRC2017) 205 (2017).

[4] L. Pacini and Y. Akaike for the CALET Collaboration, in proceedings of *The 35th International Cosmic Ray Conference*, PoS (ICRC2017) 163 (2017).

[5] N. Cannady for the CALET Collaboration, in proceedings of *The 35th International Cosmic Ray Conference*, PoS (ICRC2017) 720 (2017).

[6] M. Mori for the CALET Collaboration, in proceedings of *The 35th International Cosmic Ray Conference*, PoS (ICRC2017) 637 (2017).

[7] P.S. Marrocchesi for the CALET Collaboration, in proceedings of *The 35th International Cosmic Ray Conference*, PoS (ICRC2017) 156 (2017).

[8] Y. Akaike for the CALET Collaboration, in proceedings of *The 35th International Cosmic Ray Conference*, PoS (ICRC2017) 181 (2017).

[9] B.F. Rauch et al., *ApJ*, **697** (2009) 2083-2088, [arXiv:0906.2021].

[10] R.P. Murphy et al., *ApJ*, **831** (2016) 2083-2088, [arXiv:1608.08183].

[11] W.R. Binns et al., in proceedings of *The 33rd International Cosmic Ray Conference (Rio de Janeiro)*, (2013), paper 0646, http://www.cbpf.br/ icrc2013/papers/icrc2013-0646.pdf.

[12] J.J. Engelmann et al., *A&A*, **233** (1990) 96-111.

[13] K. Lodders, *ApJ*, **591** (2003) 1220-1247.

[14] T. Sanuki et al., *ApJ*, **545** (2000) 148-155, [arXiv:astro-ph/0002481].

[15] M. Aguilar et al., *ApJ*, **736** (2011) 105-116, [arXiv:1106.2269].

[16] S. Ozawa and Y. Asaoka for the CALET Collaboration, in proceedings of *The 35th International Cosmic Ray Conference*, PoS (ICRC2017) 165 (2017).

[17] Y. Asaoka et al., *APh*, **91** (2017) 1-10.

[18] Y. Komiya and G. Bigongiari for the CALET Collaboration, in proceedings of *The 35th International Cosmic Ray Conference*, PoS (ICRC2017) 206 (2017).

[19] R. Miyata and the CALET Collaboration, in proceedings of *The 35th International Cosmic Ray Conference*, PoS (ICRC2017) 207 (2017).

[20] P. Maestro and N. Mori for the CALET Collaboration, in proceedings of *The 35th International Cosmic Ray Conference*, PoS (ICRC2017) 208 (2017).

[21] P.S. Marrocchesi et al., *NIMPA*, **659** (2011) 477-483.

[22] C. Störmer, *The Polar Aurora*, Oxford University, London 1950.

[23] D.F. Smart & M.A. Shea, *AdSpR*, **44** (2009) 1107-1123.

[24] B.F. Rauch for the CALET Collaboration, in proceedings of *The 34th International Cosmic Ray Conference*, PoS (ICRC2015) 627 (2015).